Equation (4.50) now becomes Eq. (4.45). Thus the difference between Anderson's treatment and that of the present paper lies in the difference in the two sets of definitions of $G(x)$ and $F(x)$. Note that Eqs. (4.46)–(4.49) still hold true in the Anderson treatment.

*Work supported by the U. S. Office of Naval Research under Contract No. N00014-67-A-0209-0007.

[1]R. H. Parmenter, Phys. Rev. B 1, 2191 (1970). We refer to this paper as I.
[2]P. W. Anderson, Phys. Rev. 124, 41 (1961).
[3]R. H. Parmenter, Phys. Rev. B 1, 1071 (1970).
[4]The generalized effective field was introduced implicitly through the approximation expressed by Eq. (2.18) of I.
[5]J. Hubbard, Proc. Roy. Soc. (London) A276, 238 (1963); A281, 401 (1964).
[6]R. H. Parmenter (unpublished). We refer to this paper as II.
[7]See, e.g., R. H. Parmenter and W. R. Henson, Phys. Rev. B 2, 140 (1970).
[8]J. Bardeen, L. N. Cooper, and J. R. Schrieffer, Phys. Rev. 108, 1175 (1957).
[9]J. R. Schrieffer and P. A. Wolff, Phys. Rev. 149, 491 (1966).

PHYSICAL REVIEW B VOLUME 3, NUMBER 5 1 MARCH 1971

Field Dependence of the Magnetization and Spin-Wave Correlations in Ferromagnetic $CrBr_3$ †

C. H. Cobb and V. Jaccarino
Department of Physics, University of California, Santa Barbara, California 93106

and

J. P. Remeika
Bell Telephone Laboratories, Murray Hill, New Jersey 07971

and

Richard Silberglitt
Brookhaven National Laboratory, Upton, New York 11973

and

H. Yasuoka*
Department of Metal Sciences and Technology, Kyoto University, Kyoto, Japan

(Received 19 October 1970)

Using the Cr^{53} NMR, the field dependence of the magnetization $M(T_0, H)$ at elevated temperatures of single-crystal ferromagnetic $CrBr_3$ has been determined. While an accurate fit to the $M(T_0, H)$-vs-H data can be obtained using a two-exchange-parameter first-order renormalized spin-wave theory, the parameters required differ appreciably from those required for an accurate fit to the previously obtained $M(T, 0)$-vs-T data with the same theory. A t-matrix two-parameter–model theory, correct to lowest order in the magnon density, but to all orders in the magnon-magnon interaction, was constructed. Although both the first-order and t-matrix corrections to the spin-wave energies are sizable, the full t-matrix results only change the large first-order corrections to $M(T, H)$ by 15%. However, even if one employs the full t-matrix renormalization there are no pairs of values of the two exchange parameters which simultaneously fit the $M(T, 0)$-vs-T and $M(T_0, H)$-vs-H data. We attribute the inability of the more sophisticated theory to provide agreement with measurements of more than one thermodynamic function to be an inadequacy of the two-parameter model rather than an intrinsic failure of the theoretical approach.

I. INTRODUCTION

$CrBr_3$ is one of the few ferromagnetic insulators.[1] The study of its magnetic properties has made possible detailed comparisons of experiment with the predictions of spin-wave theory for a Heisenberg ferromagnet.[2–4] Until recently, precise measurements of the temperature dependence of the magnetization using nuclear-magnetic-resonance (NMR) techniques have been confined to the case of no external magnetic field because of the difficulty in growing large single crystals.

A series of NMR studies have been made on a $CrBr_3$ single crystal which give information on the magnetization processes and the mechanisms involved in the enhancements of the NMR signals that

are observed. In this first paper we give the results of an experimental and theoretical investigation of the field and temperature dependence of the magnetization $M(T,H)$ as deduced from the frequency dependence of the Cr^{53} NMR. Only the case of the external field applied parallel to the c (easy) axis of hexagonal $CrBr_3$ will be discussed here. The character of the different resonances, their angular dependence in a magnetic field, and the measured enhancement of the rf field as seen by the nuclei will be the subject of a subsequent paper.

In Sec. II details on the growth of the single crystals are presented, along with the experimental NMR results. The subsequent theoretical section presents the motivation for, and the details of, calculations of the self-energy and of the temperature and field dependence of the magnetization, using a two-exchange-parameter model, in which spin-wave correlations are taken into account. Use of the t matrix in including all orders of spin-wave interactions in the low-density limit is an integral part of this calculation. Section IV presents some conclusions concerning both the experimental and theoretical results of this paper.

II. EXPERIMENTAL DETAILS AND RESULTS

A. Sample Preparation and NMR Techniques

Tsubokawa's[1] method of growing $CrBr_3$ crystals, where Cr metal powder is brominated at about 750 °C in a stream of argon, usually results in thin platelets ranging in size from one to several thousand microns, depending largely on the deposition temperature. A $CrBr_3$ single crystal of dimensions $5\times11\times16$ mm, with the hexagonal c axis perpendicular to the largest face, was grown by the following procedure.

A reaction container, consisting of an Al_2O_3 boat about 1.0 cm deep, 1.5 cm wide, and 10.0 cm long, was loaded at one end with pure Cr metal powder of − 325 mesh particle size and was positioned in a quartz-lined tube furnace designed so that the Cr metal would be at a temperature of 750 °C while the other end would cross a temperature gradient dropping to approximately 600 °C. A container of liquid Br_2 was attached to the input end of the reaction tube, and the system was provided with stopcocks at both ends. After thoroughly purging the system with argon, the liquid bromine was warmed to about 50 °C and admitted to the system, while the Cr metal powder was slowly brought to a temperature of 750 °C. The system was kept at this temperature for three days, whereupon it was allowed to cool to room temperature and was purged with argon to remove excess Br_2. A thick piece of $CrBr_3$ was found at what had been the cooler end of the boat. This single crystal was quite stable but had to be protected from moisture to avoid decomposition.

Although it would be desirable to study a sample that is ellipsoidal in shape to eliminate inhomogeneous broadening of the resonance lines when the sample is saturated, the tendency of $CrBr_3$ to flake and deform[5] when cut discouraged us from doing this. Therefore, the crystal was used as is, for which we estimate the approximate demagnetizing factor with the field parallel to the c axis to be $N_D^{\parallel}=0.8(4\pi)$. Since the saturation magnetization of $CrBr_3$ at $T=0$ °K is $M_s=0.27$ kOe we would expect, for an external field H_0 applied parallel to the c axis, technical saturation to occur at a field of $H_s^{\parallel}=N_D^{\parallel}M_s=2.7$ kOe. We shall see that NMR studies provide an accurate measurement of $H_s^{\parallel}$ entirely in agreement with the above estimate.

At applied fields less than $H_s^{\parallel}$, Cr^{53} NMR is observable using marginal oscillators, superregenerative oscillators, and pulsed techniques. Because the enhancement of the NMR signal decreases markedly in going from the unsaturated to the saturated state of the crystal, in the case where $H_0>H_s^{\parallel}$ the Cr^{53} resonance was only observable using the two-pulse spin-echo method. The two incoherent pulses[6] were applied to a LC resonance circuit, with the detected signal passing through a broad-band amplifier before presentation on an oscilloscope. The NMR frequencies were measured by monitoring the position of the zero beat caused by mixing the echo and the signal from a VHF signal generator and are accurate to at least 3 parts in 10^4. To obtain the desired temperature the sample was immersed in either liquid helium or hydrogen with the pressure above the liquid properly adjusted. The resonance coil was external to the Dewar containing the sample and the cryogenic fluids.

Measurements of T_2 as a function of magnetic field show that T_2 varies by less than 6% in the range 0–6 kOe with $T_2\sim75$ μsec at 1.4 °K. The center of the resonance was determined by varying the transmitter frequency and optimizing the echo amplitude at fixed pulse separation $\tau=40$ μsec, and recovery of the receiver after the second pulse precludes measurement of echo amplitudes at times $t<18$ μsec. With $H_0>H_s^{\parallel}$ the frequency of the transmitter and the pulse separations could be fixed, and the line profile could also be examined by varying the magnetic field.

B. Observations

In zero field and at temperatures from 0.04 to $0.13T_c$ (i.e., 1.4–4.2 °K), two distinct Cr^{53} NMR signals have been observed.[2–4] One is a set of quadrupolar split lines identified with nuclei in the primary c-oriented domains, and the other is a more intense resonance which has been attributed

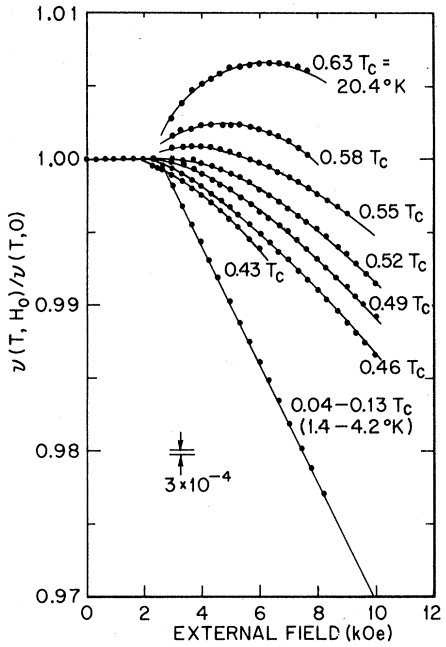

FIG. 1. Cr^{53} NMR frequency, normalized to its value at zero external field ($H_0 = 0$), plotted as a function of H_0 for various temperatures, normalized to the Curie temperature. In the lower left-hand part of the figure there is indicated the average uncertainty in the experimental measurements.

to nuclei in domains magnetized perpendicular to the c axis.[7] The character of the different resonances, their angular dependence in a magnetic field, and the measured enhancement of the rf field as seen by the nuclei will be the subject of a subsequent paper.[8] Of course, with $H_0 > H_s''$ there is only one resonance observed since all nuclei then belong to Cr^{3+} spins aligned along the direction of the applied field. In Fig. 1 we show the frequency of the central component of the quadrupolar split line ($m_I = \pm\frac{1}{2} \leftrightarrow m_{I'} = \mp\frac{1}{2}$) as a function of the external field normalized to its value $\nu(T, 0)$ at $H_0 = 0$. First, it must be made clear that with $H_0 < H_s''$ the resonance being studied is that of nuclei contained in the c-oriented domains. Second, it should be remembered that $\nu(T, 0)$ varies strongly with temperature in the region $T = 0$–$20.4\,^\circ\mathrm{K}$ ($0.63 T_C$).[4]

In the unsaturated state with $H_0 \parallel c$, the relative sizes of the up and down c-oriented domains adjust in a manner such that the external field is exactly canceled by the demagnetizing field everywhere inside the sample. What is quite remarkable is how precise is this cancellation, as is evidenced by the frequency independence of the NMR for $H_0 < H_s''$ in Fig. 1. Careful measurement shows that at a fixed temperature $\nu(T, H_0)$, for $H_0 < H_s''$, is constant to 1 part in 10^4. When $H_0 > H_s''$, the field penetrates everywhere in the sample with the effective field H_e acting on each Cr^{3+} spin equal to the external field minus the demagnetizing field:

$$H_e(T) \equiv H_0 - H_s''(T). \tag{1}$$

At low temperatures where the spontaneous magnetization of each individual Cr^{3+} spin has its maximum value, this manifests itself in the Cr^{53} NMR in that the resonance frequency shifts as a function of applied field as would a "bare" Cr^{53} nucleus in an external field H_e defined by Eq. (1) when $H_0 > H_s''$. This is clearly seen in Fig. 1 for the curve labeled 0.04–$1.3 T_C$. Notice that saturation occurs at $H_0 = 2.5$ kOe in agreement with our earlier estimate of N_D''. That the frequency shift is negative is a manifestation of the fact that the hyperfine field is negative in $CrBr_3$,[2] and the addition of the positive applied field leads to a smaller resultant field rather than a larger one.

As the temperature is increased and $\nu(T, 0)$ decreases, two effects are observed. First, the field at which penetration occurs becomes smaller since

$$H_s''(T) = N_D M(T, 0). \tag{2}$$

However, the most interesting effect is the change in the Cr^{53} NMR frequency for $H_0 > H_s''(T)$ which departs markedly from its low-temperature linear $\gamma^{53}(H_0 - H_s'')$ behavior, a direct result of the field-induced increase in the Cr^{3+} spin magnetization. This paramagnetic shift may be described by the nuclear-spin Hamiltonian

$$\mathcal{H}_n = A\vec{\mathrm{I}} \cdot \langle \vec{\mathrm{S}} \rangle_{T, H_e} + \gamma^{53} \vec{\mathrm{I}} \cdot \vec{\mathrm{H}}_e(T), \tag{3}$$

where $\langle \vec{\mathrm{S}} \rangle_{T, H_e}$ is the thermal average of the Cr^{3+} spin magnetization at temperature T in a field H_e and where $H_e(T)$ is defined by Eq. (1). Here A is the hyperfine coupling constant and is assumed to be independent of temperature. In the Appendix, consideration of the effects of A being a function of temperature will be given. The frequency for resonance is then

$$\nu(T, H_0) = \nu(T, 0) + (A/h)\langle \delta S \rangle_{T, H_e} - \gamma^{53} H_e(T) \tag{4}$$

for $H_0 > H_s''(T)$, where $\nu(T, 0) = (A/h)\langle S \rangle_{T, 0}$. As a function of applied field the fractional change in the frequency, which is the quantity shown in Fig. 1, may be expressed as

$$\frac{\nu(T, H_0)}{\nu(T, 0)} = 1 + \frac{\Delta M(T, H_e(T))}{M(T, 0)} - \frac{\gamma^{53} H_e(T)}{\nu(T, 0)}. \tag{5}$$

The last two terms in Eq. (5), which are absent for $H_0 < H_s''(T)$, are separately plotted in Fig. 2 for $T = 18\,^\circ\mathrm{K}$ ($0.55 T_C$). At this temperature $\Delta M(T, H_e)$ initially increases more rapidly with field than does the $\gamma^{53} H_e(T)$ term. However, above a field of $H_e \simeq 4$ kOe just the reverse is true, and we obtain the behavior that is evident in Fig. 1 for $\nu(T, H_0)/$

$\nu(T, 0)$.

III. THEORETICAL ANALYSIS

A. Hexagonal Model Lattice

In the previous theoretical analyses[2-4,9] of $CrBr_3$ NMR data, the hexagonal DO_5 lattice was replaced by the hexagonal model lattice shown in Fig. 3(b). This model lattice was introduced in Ref. 2, and is characterized by two exchange parameters, J_T between chromium pairs in the same hexagonal layer, and J_L between pairs in adjacent layers. Initially we will use this model lattice in the following theoretical discussion despite the fact that recent neutron scattering measurements[10] have shown five exchange constants are required to fit the full spin-wave dispersion in $CrBr_3$.

This simplification has several obvious motivations. As we have noted, all of the comparisons[2,4,9] between theory and experiment in $CrBr_3$ to date have been made using the two-exchange-parameter model. Since we have measured a different thermodynamic function, we would first like to see if the model has equal applicability, using

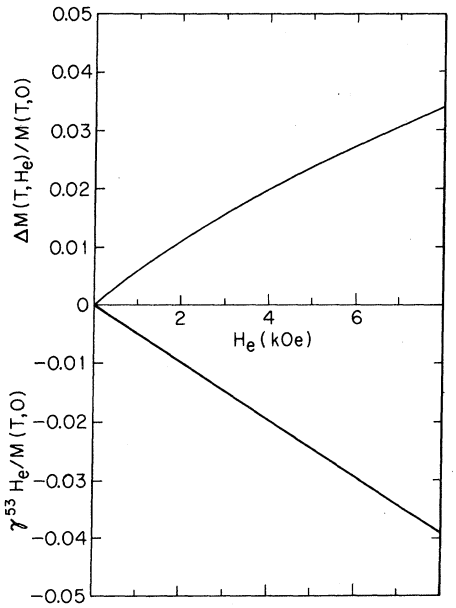

FIG. 2. Theoretical deviation of the magnetization as a function of $H_e \equiv H_0 - H_S$, normalized to the magnetization at $H_e = 0$, is shown in the upper part of the figure. The NMR frequency shift which results from the external field, normalized to the magnetization at $H_e = 0$, is shown in the lower part of the figure. It is the algebraic sum of these quantities which result in the experimental effects shown in Fig. 1. The curves are drawn for the following values of the parameters: $J_T = 8.25\,^\circ$K, $J_L = 0.497\,^\circ$K, and $T = 18\,^\circ$K.

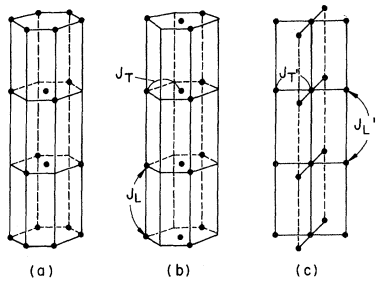

FIG. 3. Model lattices used in the study of the thermodynamics of the Cr^{3+} spins in $CrBr_3$. (a) The true $DO_5 CrBr_3$ lattice. (b) The hexagonal model lattice of Ref. 2. (c) A rectangular model lattice used in the present paper and in Ref. 9.

the previously determined J_T and J_L, to our new experimental result. Second, we might expect the model to be qualitatively correct for long-wavelength magnons in the basal plane and quantitatively correct for all magnons propagating along the c axis since the low-temperature thermodynamics is dominated by precisely these spin waves. Third, because we were interested in calculating the multiple scattering of magnons, for which a prodigious amount of computing effort is required even in a simplified two-exchange-parameter model, we felt it ill advised to investigate the thermodynamic properties of the more complicated real lattice without an initial attempt to estimate the importance of spin-wave correlations. In Sec. IV we will return to the appropriateness of this or equivalent two-parameter models as regards spin-wave correlations and the comparison to be made between experiment and theory.

B. Spin-Wave Theory for Hexagonal Model Lattice

The Hamiltonian appropriate to the hexagonal model lattice is

$$\mathcal{H} = \mathcal{H}_A - 2J_T \sum_{\langle i,j \rangle} \vec{S}_i \cdot \vec{S}_j - 2J_L \sum_{(i,j)} \vec{S}_i \cdot \vec{S}_j \,, \tag{6}$$

where $\langle\ \rangle$ and $(\ )$ denote, respectively, nearest neighbors in the same and adjacent layer perpendicular to the easy (z) direction, J_T and J_L are the exchange constants, and $\mathcal{H}_A$ is the anisotropy Hamiltonian. Davis and Narath (DN)[4] have given the expression for the spin-wave energies for this model

$$\epsilon_k^{\pm}(T) = g\mu_B H_A(T) + 6J_T S[1 \pm (\gamma_k \gamma_{-k})^{1/2}] + 4J_L S(1 - \gamma_k'), \tag{7}$$

where the $\pm$ denotes the optical and acoustic branches, respectively, that result from the presence of two inequivalent sites, and the anisotropy has been treated as an effective field $H_A(T)$. The latter is obtained from the ferromagnetic resonance data

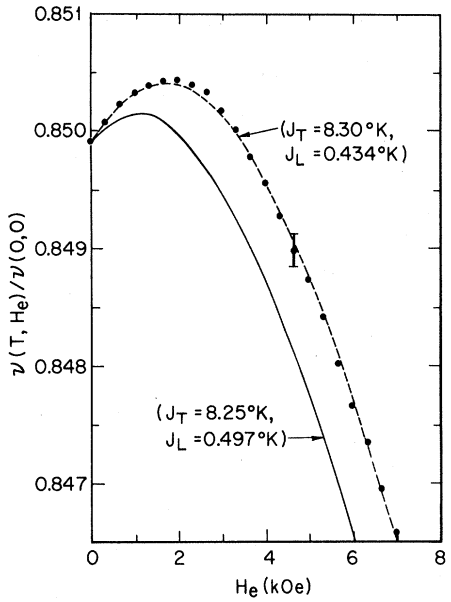

FIG. 4. Comparison of the experimental observations, at $T = 18\,°K$, for the field dependence of the NMR frequency with the results of the first-order renormalized spin-wave theory. The solid line represents the prediction of the theory for those values of the exchange parameters which give a best fit to the temperature dependence of the magnetization at zero field. The dashed line represents the prediction of the theory for a set of parameters which give a best fit to the field dependence of the magnetization at $T = 18\,°K$. The dots represent the experimental observations.

of Dillon.[11] DN calculated the spin-wave renormalization self-consistently to first order in the interaction for the model lattice. So impressive was their theoretical fit to their NMR data on $M(T, 0)$ for $T \lesssim 20\,°K$ $(0.63T_C)$ that they were able to bound the exchange constants as follows: $J_T = (8.25 \pm 0.10)\,°K$ and $J_L = (0.497 \pm 0.013)\,°K$. However, as we have noted earlier,[9] the DN first-order theory,[4] with these values of J_T and J_L, fails to describe the field dependence of the magnetization. This striking disagreement is illustrated in Fig. 4, where we have plotted both the experimental data for $\nu(18\,°K, H_e)/\nu(18\,°K, 0)$ vs H_0 and the prediction of the first-order theory.[12] It is interesting to note that a satisfactory fit to the field-dependent data with the first-order theory *can* be obtained with different values for the exchange parameters; namely, $J_T = 8.30\,°K$, $J_L = 0.434\,°K$ as indicated by the dashed line in Fig. 4. However, now the agreement between theory and experiment for $M(T, 0)$ no longer exists since the smaller value of J_L required causes $M(T, 0)$ to decrease more rapidly with increasing temperature. In fact, we have found that there are many sets of exchange constants which separately give satisfactory fits to either $M(T, 0)$ vs T or $M(18\,°K, H)$ vs H_0 but it is not possible, within the first-order theory, to fit both the temperature and field dependence of the magnetization of $CrBr_3$ with any *single* set of exchange constants. This is illustrated in the J_T-vs-J_L plot of Fig. 5, where the loci of good fits to these two thermodynamic functions are given.

One might think of a number of factors that might contribute directly or indirectly to the discrepancy between the first-order theory and the experimental results. For example, (a) magnetostriction might cause the hyperfine and/or the exchange constants to explicitly depend on the external field; (b) both of the "constants" might depend on temperature through the harmonic or

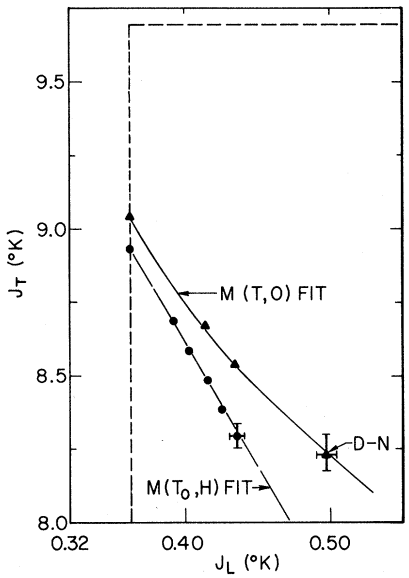

FIG. 5. Sets of exchange parameters (J_T, J_L) in the two-parameter first-order renormalized spin-wave theory which, in varying degrees of precision, "fit" the experimental observations. The circles represent values of (J_T, J_L) which fit the field dependence of the magnetization at $T = 18\,°K$. The triangles represent values of (J_T, J_L) which fit the temperature dependence of the magnetization at zero field. The dashed lines represent the bounds on J_T and J_L obtained from the magnetization measurements at lower temperatures (i.e., the linear spin-wave region). The point indicated as DN is that obtained in Ref. 4 as the best fit to the $M(T, 0)$ data. The other points on the curve give increasingly poorer fits to the same data. Similarly, the point with the indicated error bars on the lower $M(T_0, H)$ curve is the best fit obtained for our data, and likewise the fit becomes increasingly poorer as one goes in either direction away from this particular point. The curves for the two thermodynamic quantities $M(T, 0)$ and $M(T_0, H)$ do not intersect, implying that no unique set of exchange parameters exists which simultaneously provides a fit to both thermodynamic functions.

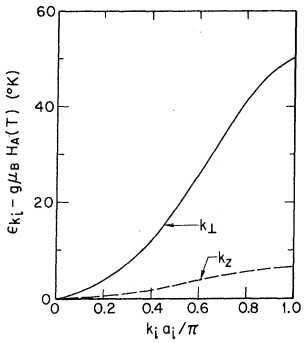

FIG. 6. Spin-wave dispersion for the hexagonal model [Fig. 3(b)] with values of the parameters J_T and J_L appropriate to $CrBr_3$. The value of ϵ_k at $k=0$ has been subtracted from all ϵ_k and the wave vectors normalized to the Brillouin-zone-boundary values in the two directions. The z direction is along the hexagonal easy axis, and the $\perp$ direction is the plane perpendicular to the easy axis. Only the acoustic branches are shown.

anharmonic vibrations of the lattice; (c) assuming neither the field nor the temperature caused measurable changes in parameters that characterize the hyperfine or exchange interaction, one could still question the accuracy of the two-parameter model in describing the true excitations of the $CrBr_3$ spin system. It could be fortuitous that, with the flexibility of adjusting both of the exchange parameters, the first-order theory applied to the approximate model is capable of fitting *one* thermodynamic function precisely – but not two; (d) last, it is entirely possible that the model is adequate but that in neglecting spin-wave correlations, by stopping at first order, we still have only an approximate theory.

The first two points are discussed in the Appendix; suffice it to say here that we do not believe magnetostriction or inconstancy of the interactions to be at the root of the discrepancy. Concerning the accuracy of the two-parameter model, we will have more to say after full consideration is given to the investigation of the importance of spin-wave correlation effects, which we now discuss.

By far the most unusual property of ferromagnetic $CrBr_3$ is the flatness of the magnon dispersion relation along the c axis. This is illustrated in Fig. 6, where we give the spin-wave energy [Eq. (7)] vs wave vector for the acoustic branch with the DN values of the exchange constants $(J_T, J_L) = (8.25,\ 0.497)$ °K. Since the Curie temperature $T_C = 32.5$ °K is large compared to the c-axis zone-boundary magnon energy, even at relatively low temperatures there is a substantial population of spin-wave states with large k_z. Now it is well known for three-dimensional systems with a single exchange constant that although long-wavelength spin waves interact only weakly,[13] those of short wavelength interact strongly, and can even form bound or resonant states.[14] For these short-wavelength magnons, first-order perturbation theory in the magnon-magnon interaction is a poor approximation; in fact, the perturbation series diverges.[15] DN recognized for $CrBr_3$ that the presence of these short-wavelength c-axis magnons at $T \ll T_C$ both invalidates the long-wavelength expansion used in Ref. 2, and leads to the strong first-order renormalization they obtained. However, the very fact that the renormalization effects obtained from the first-order theory are substantial in turn casts doubt on the adequacy of a first-order calculation. To investigate this point we have constructed a theory of the spin-wave interactions which is correct to lowest order in the spin-wave density, but to *all* orders in the interaction. The full summation of the Born series (of which the DN theory includes only the first term) is accomplished via the two-spin-wave t matrix.[15]

C. Rectangular Lattice and t-Matrix Theory

Before describing the t-matrix theory, we note two interesting aspects of the first-order theory.[4] First, if we slightly adjust the choice of values assumed for J_T and J_L, we find that self-consistency may be neglected and a fit to $M(T, 0)$ vs T obtained comparable to the DN result. Second, if we replace the Gossard, Jaccarino, and Remeika (GJR)[2] model lattice by a two-parameter *rectangular* model of the lattice [see Fig. 3(c)] with an effective $J_T' = \frac{3}{4} J_T$ and an appropriately chosen reciprocal-lattice volume, we are again able to achieve excellent agreement with the $M(T, 0)$ data. These results are illustrated in Fig. 7. Now it is not surprising that the self-consistency corrections may be neglected since they are of higher order in the magnon density. However, the magnetization has deviated by only 20% from its saturation value even at $T = 20$ °K $(0.63 T_C)$ which would indicate that the magnon density is relatively low in the temperature range of interest. We will discuss this point further in Sec. IV. The reason that the rectangular model is as adequate as is the GJR model in reproducing the $M(T, 0)$ results stems from the fact that the dominant transverse thermal excitations have characteristically small k_x and k_y; hence, their energies are reasonably well represented in the $k_x^2 + k_y^2$ approximation. It is fortunate that both of these simplifications yield results as good as those obtained by DN, since the t-matrix renormalization for the original two-sublattice hexagonal model would be exceedingly difficult to compute, particularly so if one would require self-consistency.

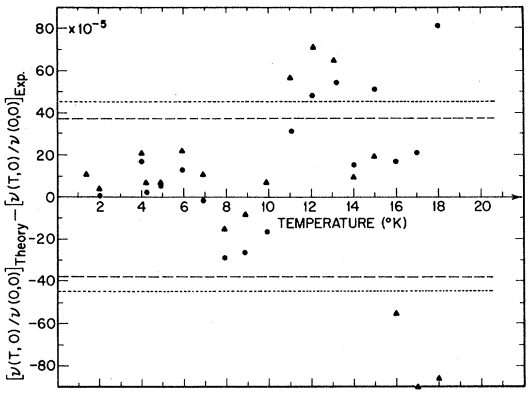

FIG. 7. Comparison of the fits obtained to the temperature dependence of the NMR frequency using a first-order renormalized theory based on a hexagonal model lattice and a rectangular model lattice. So good is the theoretical fit for either of the two models that only the differences between experiment and theory can be shown. The difference between the theoretical values for the temperature dependence of the NMR frequency $\nu(T, 0)$, normalized to its zero-temperature value, and the corresponding experimental observations of $\nu(T, 0)$ is plotted as a function of temperature. The dots indicate the theory for the hexagonal model lattice [Fig. 3(b)] and the triangles the same theory for the rectangular model lattice [Fig. 3(c)]. The rms errors for each case are shown as the dashed and dotted lines, respectively. The values of the exchange parameters used were $J_T = 8.25\,^\circ\mathrm{K}$, $J_L = 0.497\,^\circ\mathrm{K}$ (hexagonal), and $J_T' = \frac{3}{4}J_T$, $J_L' = J_L$ (rectangular).

The Hamiltonian for the rectangular model is

$$\mathcal{H} = \mathcal{H}_A - 2J_T' \sum_{\langle i,j \rangle} \vec{S}_i \cdot \vec{S}_j - 2J_L' \sum_{(i,j)} \vec{S}_i \cdot \vec{S}_j \,. \tag{8}$$

We use the Dyson-Maleev boson representation for the spin operators[4,13,16]

$$S_i^+ = (2S)^{1/2} a_i^\dagger [1 - (a_i^\dagger a_i/2S)], \qquad S_i^- = (2S)^{1/2} a_i, \qquad S_i^z = -S + a_i^\dagger a_i. \tag{9}$$

With the Fourier transformation

$$a_k^\dagger = \frac{1}{\sqrt{N}} \sum_{\vec{x}_i} e^{i\vec{k}\cdot\vec{x}_i} a_i^\dagger \,,$$

the Hamiltonian, Eq. (8), becomes

$$\mathcal{H} = \mathcal{H}_A + E_0 + \sum_k \epsilon_k a_k^\dagger a_k + \frac{1}{N} \sum_{k_1,k_2,q} V(k_1 k_2 q) \times a_{q/2+k_2}^\dagger a_{q/2-k_2}^\dagger a_{q/2+k_1} a_{q/2-k_1} \,, \tag{10}$$

where

$$V(k_1 k_2 q) = -4 \sum_{\delta=xyz} J_\delta' \cos(\vec{k}_1 \cdot \vec{\delta}) \times [\cos(\vec{k}_2 \cdot \vec{\delta}) - \cos(\tfrac{1}{2}\vec{q} \cdot \vec{\delta})], \tag{11}$$

and the spin-wave energy in this model is

$$\epsilon_k = g\mu_B H_A(T) + 6J_L(1 - \cos k_z a') + 9J_T[1 - \tfrac{1}{2}\cos(k_x a) - \tfrac{1}{2}\cos(k_y a)]. \tag{12}$$

At finite temperatures we calculate the irreducible spin-wave self-energy[17] $\sum_k(\epsilon_k)$ whose real part gives the spin-wave energy shift and whose imaginary part gives the energy width.[18] To calculate the self-energy one must consider all irreducible diagrams in which a single magnon line both enters and leaves, undergoing all possible scatterings via $V(k_1 k_2 q)$ in intermediate states. Here irreducible means that a self-energy diagram cannot be broken into two self-energy diagrams by cutting a single line.[17] It is well known[19] that if one orders Feynman diagrams according to the number of backward lines, an expansion in the density of particles is obtained. In the case of the spin-wave self-energy the sum of all the one-backward-line diagrams yields the full contribution to lowest order in the density of spin waves. This calculation correctly gives Dyson's T^4 term in the magnetization.[15] In Fig. 8(a) we show the series which when summed yields the full one-backward-line contribution to the self-energy. Although the first-Born approximation of Ref. 4 corresponds to including only the first term[20] of this series, we will sum the full series via the t matrix. The integral equation for the t matrix which may be deduced from Fig. 8(b) is

$$t(k_1 k_2 q\omega) = V(k_1 k_2 q) + \frac{1}{N} \sum_{k_3} \frac{V(k_3 k_2 q)\, t(k_1 k_3 q\omega)}{\omega - \epsilon_{q/2+k_3} - \epsilon_{q/2-k_3} + i\eta} \,, \tag{13}$$

where $\eta \to 0^+$. Since the potential is a sum of separable terms, Eq. (13) may be solved algebraically to yield

$$t(k_1 k_2 q\omega) = -4 \sum_{\delta,\delta'=xyz} J_\delta' \cos(\vec{k}_1 \cdot \vec{\delta}) \times [\cos(\vec{k}_2 \cdot \vec{\delta}') - \cos(\tfrac{1}{2}\vec{q} \cdot \vec{\delta}')][\vec{1} - 2\vec{A}]^{-1}_{\delta'\delta} \,, \tag{14}$$

where

$$A_{ij}(q\omega) = -\frac{2}{N} \sum_k \frac{J_i' \cos k_i (\cos k_j - \cos \tfrac{1}{2} q_j)}{\omega - \epsilon_{q/2+k} - \epsilon_{q/2-k} + i\eta} \,. \tag{15}$$

The matrix $\vec{A}(q, \omega)$ may be computed via the same kind of numerical analysis as is described in Ref. 15, with the added complication that since $J_L' \neq J_T'$, there are five rather than two elements even in the highest-symmetry case $q_x = q_y = q_z$. Quite generally the magnetization is obtained from the relation

$$M = NS + (1/\pi) \int d\omega \sum_k (e^{\beta\omega} - 1)^{-1} \mathrm{Im}[\omega - \epsilon_k - \Sigma_k(\omega)]^{-1} \,. \tag{16}$$

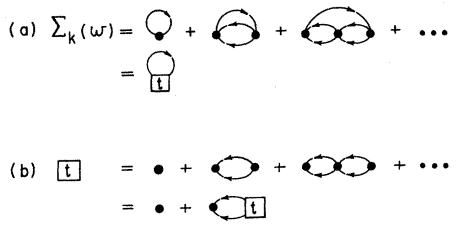

FIG. 8. Diagrammatic representations of the full contribution to the magnon self-energy and t matrix to lowest order in the density of spin waves. The self-energy (a) is the sum of all one-backward-line diagrams. The t matrix (b) contains only those diagrams with no backward lines. In the diagrammatic representation, each backward line corresponds to a factor of the density of spin waves. The first term on the right-hand side is the Born approximation for Σ_k or t.

We calculate the self-energy[21]

$$\Sigma_k(\omega) = (2/N)\sum_p (e^{\beta\epsilon_p} - 1)^{-1} \times t[\tfrac{1}{2}(p-k),\ \tfrac{1}{2}(p-k),\ p+k,\ \omega+\epsilon_p]. \quad (17)$$

If terms of order $[\mathrm{Im}\Sigma_k(\epsilon_k)]^2$ are neglected the magnetization is obtained from the approximate expression

$$M = NS - \sum_k (e^{\beta[\epsilon_k + \mathrm{Re}\Sigma_k(\epsilon_k)]} - 1)^{-1} . \quad (18)$$

The three-dimensional integrations required by Eqs. (17) and (18) have been performed numerically with the use of Simpson's rule; the t matrix was calculated from Eq. (14) and then tabulated for use in these integrations.

D. Numerical Results and Comparison with Experiment

a. Self-energy. As we have noted previously,[9] the inclusion of repeated scatterings [diagrammatically indicated in Fig. 8(a)] results in significant corrections to the first-order self-energy at elevated temperatures. We have investigated the dependence of $\mathrm{Re}\Sigma_k(\epsilon_k) \equiv \Sigma'_k(\epsilon_k)$ on k_z and $k_\perp$ ($k_\perp \equiv k_x \equiv k_y$). The behavior is displayed in the two parts of Fig. 9 which are representative of the results of many numerical calculations. There are some notable features to the dependence of $\Sigma'_k(\epsilon_k)$ on k_z and $k_\perp$. For fixed $k_\perp$ we observe that [see Fig. 9(a)] the differences between the first-order and full t-matrix calculations are largest for k_z somewhere between $\frac{2}{3}k_z^{\max}$ and $\frac{3}{4}k_z^{\max}$, a behavior reminiscent of the three-dimensional system, with a single exchange interaction, for $\vec{k} = k(1,1,1)$.[15]

When k_z is fixed one finds [see Fig. 9(b)] that the t-matrix self-energy first decreases and then increases as $k_\perp$ increases in magnitude, with the *differences* between the first-order and full t-matrix calculations displaying a distinct minimum for $0.05 < k_\perp a/\pi < 0.1$. This unexpected behavior can be attributed to the fact that $J_T \gg J_L$, so that as $k_\perp$ increases the transverse part of the energy spectrum becomes increasingly important. Thus the large correlation effects in the longitudinal direction are de-emphasized as $k_\perp$ increases, leading to the minimum at about $0.1\, k_\perp^{\max}$. Finally, for large $k_\perp$, the transverse spectrum begins to renormalize substantially and then the differences between the two calculations do increase with increasing $k_\perp$. However, those spin waves with $k_\perp$ near the minimum in Fig. 9(b) are certainly thermodynamically important for $T \simeq 15$–$20\,^\circ$K. Therefore, the depression of $\Sigma'_k(\epsilon_k)$ arising from the cancellation described above will cause the effect of correlations on thermodynamic quantities to be smaller than might be expected from Fig. 9(a) alone. Consequently, although there are deviations in $\Sigma'_k(\epsilon_k)$ from the first-order theory that are as large as 40–50% for particular values of k, corrections to $M(T_0, H)$ result which are only of order 10–15%.

b. $M(T, 0)$. Calculations of the magnetization

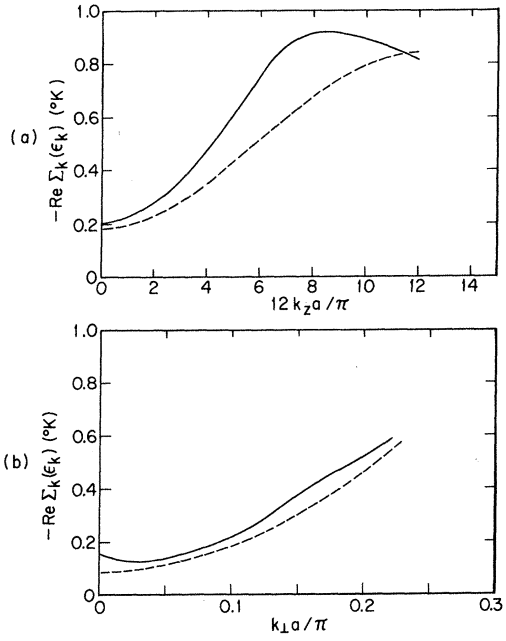

FIG. 9. Real part of the magnon self-energy Σ'_k as a function of the wave vector k, in two symmetry directions, for the rectangular model [Fig. 3(c)]. The solid lines are obtained from the full t-matrix theory which is correct to all orders in the magnon-magnon interaction, while the dashed lines result from only including magnon interactions in the lowest order. (a) Σ'_k vs k_z for $k_\perp a = \frac{1}{7}\pi$. Note that the difference between the first-order and full t-matrix results are largest for $k_z a$ about 0.7π. (b) Σ'_k vs $k_\perp$ for $k_z a = \frac{3}{12}\pi$. The difference between the first-order and full t-matrix calculations displays a distinct minimum for $0.05 < k_\perp a/\pi < 0.1$.

for a given temperature using Eq. (18) involve a considerable amount of computing time. They become prohibitively expensive if a full plot of $M(T,0)$ vs T is required. Instead, we have made a comparison in Table I of the results obtained from the linear spin-wave, first-order, and full t-matrix renormalization theories at a fixed temperature ($T=18\,^\circ$K) for a specific set of values of J_T' and J_L'; namely, the ones for which a good fit to $M(T,0)$ vs T for $CrBr_3$ is obtained using the first-order theory (see Fig. 5).

The table illustrates the following points, some of which have been made previously.[9] The first-order theory produces large corrections in the magnetization at elevated temperatures to that obtained from the linear theory, although making the former calculation self-consistent appears less important. A further sizable decrease in $M(T,0)$ is obtained from carrying the renormalization to infinite order but it is less than the difference between the linear and first-order renormalized spin-wave results. The size of the differences between the linear theory and the first-order and full t-matrix results are consistent with the magnitudes of $\Sigma_k'(\epsilon_k)$ for the two renormalization procedures and the observations made above.

c. $M(T_0,H)$. A perhaps not surprising similarity appears between the predicted behavior for $M(18\,^\circ\text{K},H)$ vs H, for the various theories, and the calculated results for $M(T,0)$ vs T at $H=0$. The first-order theory produces sizable corrections to the linear theory although, once more, self-consistency is of little importance. The full t-matrix theory yields an increased susceptibility over and beyond that given by the first-order theory although the difference between the full t-matrix and first-order theories is only 15% of the difference between the first-order and linear spin-wave theories. The reasons for this are again related to the discussion following Fig. 9.

However, one inescapable result of the comparison between experiment and the t-matrix renormalization theory is that still *there are no pairs of values of* J_L' *and* J_T' *which simultaneously fit the* $CrBr_3$ $M(T,0)$*-vs-*T *and* $M(18\,^\circ\text{K},H)$*-vs-*H *data*, as was noted to be the case previously for the first-order theory. This is not to say that a truly excellent fit to either set of data cannot be had with a particular set J_L' and J_T', but that the best fit to one or the other of the thermodynamic function requires sets of values for which the J''s differ by as much as 10–15%.

We attribute this inability of the more sophisticated theory to provide detailed agreement with measurements of more than one thermodynamic function to the inadequacy of the two-parameter model for $CrBr_3$ rather than an intrinsic failing of the theoretical approach. In fact, evidence for the limitation of the two-parameter approach has been recently obtained[10] from inelastic neutron scattering studies of the spin-wave dispersion throughout the Brillouin zone. Analysis of the neutron data indicates that five parameters are necessary to properly specify the spin-wave dispersion. With the five-parameter model an excellent least-squares fit was obtained for all the acoustic spin-wave modes. The insufficiency of the two-parameter model manifests itself insofar as the dispersion in the (k_x,k_y) plane can be fitted by a two-parameter model for a particular value of k_z, but the parameter J_T required to achieve a good fit changes by

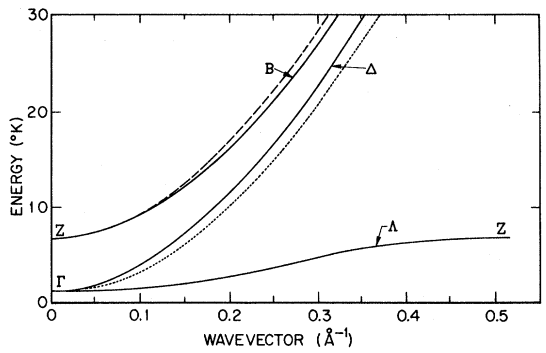

FIG. 10. Dispersion of spin waves of low energy in $CrBr_3$, in three symmetry directions, as obtained from inelastic neutron scattering (Ref. 10). The solid lines labeled Λ and Δ have as their origin the Γ point of the Brillouin zone. The solid line Δ corresponds to dispersion in the basal plane with $k_z=0$. The solid line labeled B has the point Z of the Brillouin zone as its origin and corresponds to dispersion in the basal plane with $k_z=\pi$. The dashed line is a vertical displacement upward of the line Δ, and the dotted line is a vertical displacement downward of the line B by an energy $\epsilon(k_z=\pi)-\epsilon(k_z=0)$. Comparison of the dotted and dashed curves B and Δ shows that the basal-plane dispersion is a function of k_z. On the contrary, if a two-parameter model was appropriate, the dashed and dotted lines would coincide with B and Δ, respectively.

TABLE I. Values of the predicted fractional change in the magnetization for the rectangular ferromagnet at $T=18\,^\circ$K with $J_T'=6.19\,^\circ$K and $J_L'=0.497\,^\circ$K in the linear spin-wave, first-order (with and without self-consistency), and full t-matrix renormalization approximations.

	Linear spin wave	First order without self-consist	First order with self-consist	Full t matrix
$1-\frac{M(18\,^\circ\text{K})}{M(0)}$	0.14109	0.14954	0.15029	0.15247

10% as k_z varies from zone center to the zone boundary, as is illustrated in Fig. 10.

IV. SUMMARY AND CONCLUSIONS

Using the NMR technique the field dependence of the magnetization at elevated temperatures of ferromagnetic $CrBr_3$ has been determined. Although an accurate fit to the $M(T_0, H)$-vs-H data is obtained using a two-exchange parameter (J_T', J_L') first-order renormalized spin-wave theory, the values of J_T' and J_L' required differ appreciably from those previously obtained in fitting the $M(T, 0)$-vs-T data with the same theory. Because of this discrepancy between the fits to the two thermodynamic functions and the large corrections obtained in the first-order theory, it was felt that multiple spin-wave interactions should be considerd. A t-matrix theory, correct to lowest order in the magnon density but to all orders in the magnon-magnon interaction, was constructed. Although the numerical results obtained from the full t-matrix theory show differences from the first-order theory in the self-energy and the two thermodynamic functions which are quantitatively significant, they do not remove the discrepancy alluded to above; specifically, no two-exchange parameter fitted to *both* thermodynamic functions is obtainable with a single pair of values for J_T' and J_L'. This result is consistent with recent inelastic neutron scattering experiments which indicate that a five-parameter model is necessary to properly describe the spin-wave dispersion in $CrBr_3$.[22]

We feel there is a valuable lesson to be learned from these studies. It is not uncommon for accurate measurements of one of the thermodynamic properties of a ferromagnet or antiferromagnet to be combined with limited information on the nature of the exchange and anisotropic spin interactions and used with a specific model Hamiltonian to obtain "precise" values for the parameters that characterize the interactions. In the sense that any thermodynamic function weights all of the elementary excitations it is not surprising that, with an approximate model, a very good fit to the experimental data may be obtained which appears to bracket the values of the parameters in some very narrow range. However, one would be wrong to assume that the values for the parameters so obtained conclusively prove the accuracy of the model or that the "precision" of the parameters has other than curve-fitting significance. Our results strongly suggest the importance of making more than one precise thermodynamic measurement on a magnetically ordered system before any judgment be rendered as to the accuracy of the model, the detailed importance of spin-wave interactions, etc. We believe $CrBr_3$ to be the first instance where sufficient information has become available to see that this is indeed the case.

ACKNOWLEDGMENTS

The authors wish to thank Dr. M. A. Butler, Professor D. Hone, and Dr. A. Narath for many stimulating discussions.

APPENDIX

The thermodynamic quantities which are obtained from the resonance experiments $\nu(T, 0)$ vs T and $\nu(T_0, H)$ vs H suffer from the fact they *may* have a different dependence on temperature and field, respectively, than do the quantities with which comparison with theory is made, namely, the magnetizations at constant volume $M_V(T, 0)$ vs T and $M_V(T_0, H)$ vs H. We examine this problem now and estimate the size of the appropriate corrections.

As regards explicit and implicit temperature-dependent effects, we know that the anharmonicity in the lattice vibrations causes a monotonic expansion of a crystal with increasing temperature. Hence, if we desire to know the dependence of the magnetization M on T at constant atomic separation (constant exchange) we must correct measurements at constant pressure, using the relation[23]

$$\frac{1}{M}\left(\frac{\partial M}{\partial T}\right)_P = \frac{1}{M}\left(\frac{\partial M}{\partial T}\right)_V + \frac{\alpha}{K}\left(\frac{1}{M}\frac{\partial M}{\partial P}\right)_T , \tag{A1}$$

where the thermal-expansion coefficient $\alpha \equiv (1/V) \times (\partial V/\partial T)_P$ and the compressibility $K \equiv (1/V)(\partial V/\partial P)_T$. Knowledge of the pressure dependence of the magnetization as a function of temperature and α and K would suffice to correct $M_P(T)$ to $M_V(T)$. Since, in fact, what is measured is $\nu_P(T)$ and $\nu(T) \propto AM(T)$, the more general relation

$$\frac{1}{\nu}\left(\frac{\partial \nu}{\partial T}\right)_P = \frac{1}{M}\left(\frac{\partial M}{\partial T}\right)_V + \frac{1}{A}\left(\frac{\partial A}{\partial T}\right)_V + \frac{\alpha}{K}\left[\frac{1}{A}\left(\frac{\partial A}{\partial P}\right)_T + \frac{1}{M}\left(\frac{\partial M}{\partial P}\right)_T\right] \tag{A2}$$

is required to obtain $M_V(T)$ from $\nu_P(T)$. Assuming the pressure dependence of A as a function of T was obtainable, it would appear $M(T)_V$ could be determined from measurements of $\nu(T)_P$, providing $(\partial A/\partial T)_V \simeq 0$. A source of the explicit dependence of A upon T could be the dynamic orbit-lattice admixing of excited states due to the *harmonic* vibrations of the crystal.[24] The latter are proportional to the mean-square strain $\langle \epsilon \rangle^2$ and therefore to T^4 at $T \ll \Theta_D$.

None of the relevant pressure derivatives have been measured for $CrBr_3$ nor do we know α or K. However, we do know from heat-capacity measurements[25] that the Debye temperature $\Theta_D = 131\ ^\circ K$ is much larger than T_C which in turn is larger than the maximum temperature ($0.55T_C$) at which we

have made comparison between experiment and theory. When $T \simeq 0.\ \Theta_D$ or less, we would expect the harmonic corrections to A to have a $(T/\Theta_D)^4$ dependence and, since even at $T \simeq \Theta_D$ the measured changes that have been found[26] are only of order 1–5%, we might expect A^{53} to change by 0.1% or less in the temperature region of interest. Ideally, one would like to measure the temperature dependence of A^{53} in an isomorphic nonmagnetic crystal (e.g., BiI_3) with small amounts of Cr^{3+}. The anharmonic corrections are, if anything, expected to be somewhat smaller than the harmonic ones.

Inadvertently, we have determined how large would be the changes in A with T required to force a fit with field-dependent data. The quantity $\nu(T, H_0)/\nu(T, 0)$ in Eq. (5) is independent of A (assuming A does not depend on H – a result which we will show). However, $\nu(T, H_0)/\nu(0, 0)$, which for convenience was the quantity calculated in Sec. III, would have a dependence on T, other than through $M(T)$, if $A = A(T)$. Suppose $A(T) \equiv A(0)\,[1 + \delta(T)]$. Then

$$\frac{\nu(T, H_e)}{\nu(0, 0)} = [1 + \delta(T)]\ \frac{M(T, H_e)}{M(0, 0)} - \frac{\gamma^{53} H_e(T)}{\nu(0, 0)}. \qquad \text{(A3)}$$

In Sec. III we plotted Eq. (A3) assuming $\delta(T) \equiv 0$. Now in Fig. 11, Eq. (A3) is plotted as a function of $H_e(18\,^\circ\mathrm{K})$ for values of $\delta(T) \neq 0$. We see a 5% change in $A(0)$ is required before the data could be fitted, an increase we consider entirely unreasonable. Moreover, such a change would worsen the agreement between the $M(T, 0)$-vs-T data since the fit to the latter experiment was accomplished assuming $\delta(T) \equiv 0$. Therefore, we conclude that the discrepancies are just too large to be explained by a temperature dependence of A^{53} at such low temperatures.

Similar arguments may be offered for the temperature dependence of the exchange parameters upon which $M_V(T)$ implicitly depends. We have seen already in our J_T-vs-J_L plot that changes of the order of 10–15% are required in either J_T or J_L to make one of the thermodynamic functions agree with the other at a specific elevated temperature. Of course, here again if $J = J(T)$ we could not get *both* functions to agree over a range of temperatures any better than we could assuming J_L or J_T was temperature independent.

The question of the field dependence of the parameters and magnetostrictive effects, in general, is somewhat more interesting; perhaps, because the experiments speak for themselves on this point. Consider first the field dependence of A^{53} which might arise directly through an explicit dependence of A^{53} upon H (unlikely) or indirectly through a magnetostrictively induced volume dependence of A. At very low temperatures, with $H_0'' < H_s''$, we have interpreted the absence of any frequency dependence of

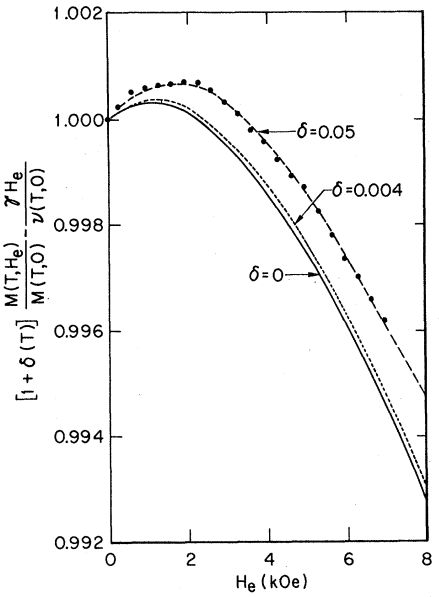

FIG. 11. Graphical representation of how large the temperature dependence of the hyperfine coupling constant A would have to be to bring experiment and theory into accord. The field dependence of the NMR frequency, normalized to its value at zero field and assuming A to be temperature dependent, is shown in the figure for various fractional changes δ in A with T. The experimental data indicated by the dots are for $T = 18\,^\circ\mathrm{K}$, and the calculated curves assume values of the exchange parameters that would fit the experimental data for $M(T, 0)$ using the first-order theory (see Ref. 4).

the resonance upon applied field (see Fig. 1) as evidence for the internal exact cancellation of the applied field by the demagnetizing field. But we know magnetostriction is very large in the unmagnetized state in ferromagnets and we might expect the size changes that are observed in macroscopic measurements would be reflected in changes in A^{53} with H. The experiments show that A^{53} changes by less than 1 part in 10^5 when H varies between 0 and $H_s'' = 2.5$ kOe. One could also argue that in the saturated state the slope of ν vs H would not be constant if magnetostriction caused A to be a function of H.

The very-low temperature data give no information on the changes in J_T and/or J_L that result from magnetostriction. The reason for this is that, when $T \ll T_C$, $\langle S_z \rangle_T \simeq S$ and small changes in J_T and/or J_L simply cannot change $\langle S_z \rangle$. However, at elevated temperatures, where $(S - \langle S_z \rangle_T)/S \simeq 20\%$, changes in J_T and/or J_L will cause $M(T)$ to change through the implicit dependence of $M(T)$ on T_C, namely, in Eq. (A1),

$$\frac{1}{M}\left(\frac{\partial M}{\partial P}\right)_T = \frac{1}{M}\left(\frac{\partial M}{\partial T_C}\right)_T \left(\frac{\partial T_C}{\partial P}\right)_T$$

$$= \frac{1}{M}\left(\frac{\partial M}{\partial T_C}\right)_T \left(\frac{\partial T_C}{\partial V}\right)_T \left(\frac{\partial V}{\partial P}\right)_T . \qquad \text{(A4)}$$

Again, for $0 \leq H_0^{\parallel} < H_s^{\parallel}$ we find the frequency of the Cr^{53} NMR to be independent of H_0 at 18 °K (see Fig. 1) indicating that the magnetostrictive effects on M are beyond our experimental sensitivity. Since we expect the magnetostrictive effects to be larger below $H_s^{\parallel}$ than above, we would argue that the high-field data need suffer no correction for magnetostrictively induced volume changes in either $M(T_0)_P$ or A^{53}. While it would certainly be desirable to measure all of the quantities in Eqs. (A2) and (A4) it seems to us that the discrepancies in the interpretation of the two measurements do not arise from the temperature and/or field dependence of the hyperfine and exchange parameters.

---

†Work at the University of California, Santa Barbara, supported in part by the National Science Foundation and that at Brookhaven National Laboratory performed under the auspices of the U. S. Atomic Energy Commission.

*Work performed in part at the University of California, Santa Barbara, Calif.

[1]I. Tsubokawa, J. Phys. Soc. Japan 15, 1664 (1960).

[2]A. C. Gossard, V. Jaccarino, and J. P. Remeika, Phys. Rev. Letters 7, 122 (1961).

[3]A. C. Gossard, V. Jaccarino, and J. P. Remeika, J. Appl. Phys. Suppl. 33, 1187 (1962).

[4]H. L. Davis and A. Narath, Phys. Rev. 134, 433 (1964).

[5]J. F. Dillon, Jr. and M. Teague, Rev. Sci. Instr. 35, 747 (1964).

[6]An Arenberg Ultrasonic Laboratory PG-650 C-pulsed oscillator modulated by a General Radio 1395-A modular pulse generator formed the incoherent pulses.

[7]C. H. Cobb, H. Yasuoka, V. Jaccarino, and J. P. Remeika, Bull. Am. Phys. Soc. 13, 473 (1968).

[8]C. H. Cobb, V. Jaccarino, H. Yasuoka, and J. P. Remeika (unpublished).

[9]R. Silberglitt, C. H. Cobb, and V. Jaccarino, J. Appl. Phys. 41, 952 (1970).

[10]E. J. Samuelsen, R. Silberglitt, G. Shirane, and J. P. Remeika, Phys. Rev. B (to be published).

[11]J. F. Dillon, J. Appl. Phys. Suppl. 33, 1191 (1962).

[12]We thank Dr. A. Narath for making his $M(T, 0)$ computer programs available to us.

[13]F. J. Dyson, Phys. Rev. 102, 1217 (1957); 102, 1230 (1957).

[14]M. Wortis, Phys. Rev. 132, 85 (1963); J. Hanus, Phys. Rev. Letters 11, 336 (1963); R. G. Boyd and J. Callaway, Phys. Rev. 138, A1621 (1965).

[15]R. Silberglitt and A. B. Harris, Phys. Rev. 174, 640 (1968).

[16]S. V. Maleev, Zh. Eksperim. i Teor. Fiz. 33, 1010 (1957) [Soviet Phys. JETP 6, 776 (1958)].

[17]A. A. Abrikosov, L. P. Gorkov, and I. E. Dzyaloshinskii, *Quantum Field Theoretical Methods in Statistical Physics*, 2nd ed. (Pergamon, New York, 1965).

[18]One should really calculate the spectral function of the spin Green's function, but if this function is sharply peaked and $\Sigma_k(\omega)$ is slowly varying near $\omega = \epsilon_k$ it is sufficient to consider $\Sigma_k(\epsilon_k)$. See Ref. 15 for explicit calculations of both quantities.

[19]R. Balian and C. De Dominicis, Nucl. Phys. 16, 502 (1960); J. M. Luttinger, Phys. Rev. 121, 942 (1961); I. E. Dzyaloshinskii, Zh. Eksperim. i Teor. Fiz. 42, 1126 (1962) [Soviet Phys. JETP 15, 778 (1962)]; G. Baym and A. M. Sessler, Phys. Rev. 131, 2345 (1963).

[20]In addition DN (Ref. 4) require self-consistency, but as we have pointed out previously these corrections make little difference.

[21]Here we have neglected the frequency dependence of the intermediate propagators. This should be a good approximation except for $\omega \to 0$.

[22]A full t-matrix calculation with the five-parameter model would be exceedingly difficult. However, an attempt is now being made to calculate the thermodynamics of the five-parameter model including spin-wave interactions in only the lowest order. We feel the results of this calculation will bring measurements of $M(T, 0)$ and of $M(T_0, H)$ into agreement for specific values of the parameter. However, the exchange parameters would necessarily not be the same ones that would obtain from a full t-matrix calculation.

[23]An excellent discussion of anharmonic corrections in magnetic-resonance experiments is given in G. B. Benedek, *Magnetic Resonance at High Pressure* (Interscience, New York, 1963).

[24]E. Simanek and R. Orbach, Phys. Rev. 145, 191 (1966).

[25]L. D. Jennings and W. N. Hansen, Phys. Rev. 139, A1694 (1965).

[26]Here we refer to the experiments on the temperature and pressure dependence of the Mn^{2+} hyperfine interaction A^{53} when Mn^{2+} is introduced substitutionally into the MgO lattice by W. M. Walsh, Jr., J. Jeener, and N. Bloembergen, Phys. Rev. 139, A1338 (1965).